ACS APPLIED MATERIALS & INTERFACES

Research Article

www.acsami.org

Ultrathin Nondoped Emissive Layers for Efficient and Simple Monochrome and White Organic Light-Emitting Diodes

Yongbiao Zhao, Jiangshan Chen, and Dongge Ma*

State Key Laboratory of Polymer Physics and Chemistry, Changchun Institute of Applied Chemistry, Chinese Academy of Sciences, Graduate University of the Chinese Academy of Sciences, Changchun 130022, People's Republic of China

ABSTRACT: In this paper, highly efficient and simple monochrome blue, green, orange, and red organic light emitting diodes (OLEDs) based on ultrathin nondoped emissive layers (EMLs) have been reported. The ultrathin nondoped EML was constructed by introducing a 0.1 nm thin layer of pure phosphorescent dyes between a hole transporting layer and an electron transporting layer. The maximum external quantum efficiencies (EQEs) reached 17.1%, 20.9%, 17.3%, and 19.2% for blue, green, orange, and red monochrome OLEDs, respectively, indicating the universality of the ultrathin nondoped EML for most phosphorescent dyes. On the basis of this, simple white OLED structures are also demonstrated. The demonstrated complementary blue/orange, three primary blue/green/red, and four color blue/green/orange/red white OLEDs show high efficiency and good white emission, indicating the advantage of ultrathin nondoped EMLs on constructing simple and efficient white OLEDs.

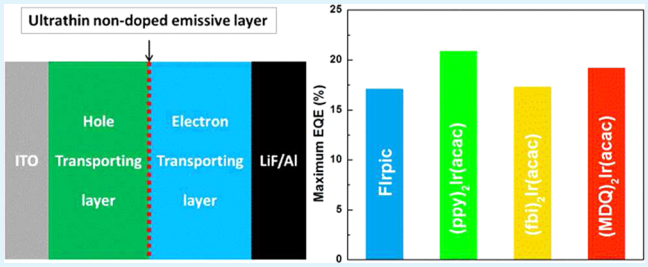

KEYWORDS: *organic light-emitting diode, white, nondoped emissive layer, ultrathin emissive layer, interface doping, simple*

INTRODUCTION

Owning to their high efficiency, light weight, and possibility for fabrication on large area flexible substrates at low cost, organic light emitting diodes (OLEDs)[1] show great potential for future full color displays and lighting sources.[2−5] During the past three decades, many useful techniques, such as host−guest doping,[6] electrode modification,[7,8] phosphorescent emitters,[9] p-doping[10,11] and n-doping,[12,13] charge/exciton confinement,[14,15] and out-coupling enhancement,[16,17] have been demonstrated, and the performance of OLEDs has been greatly improved. Now many products, such as OLEDs displays and OLEDs lighting panels, are entering the market.

To reduce the fabrication cost, there is a trend in simplifying the device structures. For example, Kim et al. demonstrated a green emitting OLEDs with only three organic materials, where the hosts in the emissive layer (EML) were the same as the transporting layers.[18] Liu et al. reported efficient red, green, and blue OLEDs with a single layer structure, where different phosphorescent dyes were doped into an electron transporting material 1,3,5-tris(*N*-phenylbenzimidazole-2-yl)benzene (TPBi).[19] However, as we can see, all of them have used doped EMLs. Later, Divayana et al.[20] and Liu et al.[21] reported OLEDs with nondoped repeated [host/guest/host/guest/...] EML structure, which can further simplify the fabrication process as there is no doping process. Though both of them have achieved improved device performance, the device structures were still a little complex. Recently, by introducing a very thin layer of orange phosphorescent dyes (as thin as 0.1 nm) between a hole transporting layer and an electron transporting layer, an orange OLED with efficiency higher than a doped EML device was reported.[22] The even simpler structure and the high efficiency indicates the importance of charge/exciton management on simplifying the OLED structures while maintain the high device performance.

As we know, in doped EML OLEDs, the host−guest combination is critical to the final device performance and it is hard to realize effective emission of different dyes with the same host materials. Thus it is of interest to check if this kind of ultrathin nondoped EML can be properly adapted by other phosphorescent dyes. In this paper, we fabricated monochrome blue, green, orange, and red phosphorescent OLEDs based on ultrathin nondoped EMLs. It is clearly seen that these ultrathin nondoped EML-based OLEDs show high efficiency, with maximum external quantum efficiency (EQE) reaching 17.1%, 20.9%, 17.3%, and 19.2% for blue, green, orange, and red devices, respectively. As a comparison, the OLEDs with doped EMLs show obvious host dependence. This indicates that the ultrathin nondoped EML can be universally adopted by other phosphorescent dyes. Furthermore, we also constructed white OLEDs with this kind of EML. The demonstrated complementary blue/orange, three primary blue/green/red, and four color blue/green/orange/red white OLEDs show high efficiency and good white emission, indicating the advantage of ultrathin nondoped EMLs on constructing simple and efficient white OLEDs.

Received: November 7, 2012
Accepted: January 16, 2013
Published: January 16, 2013

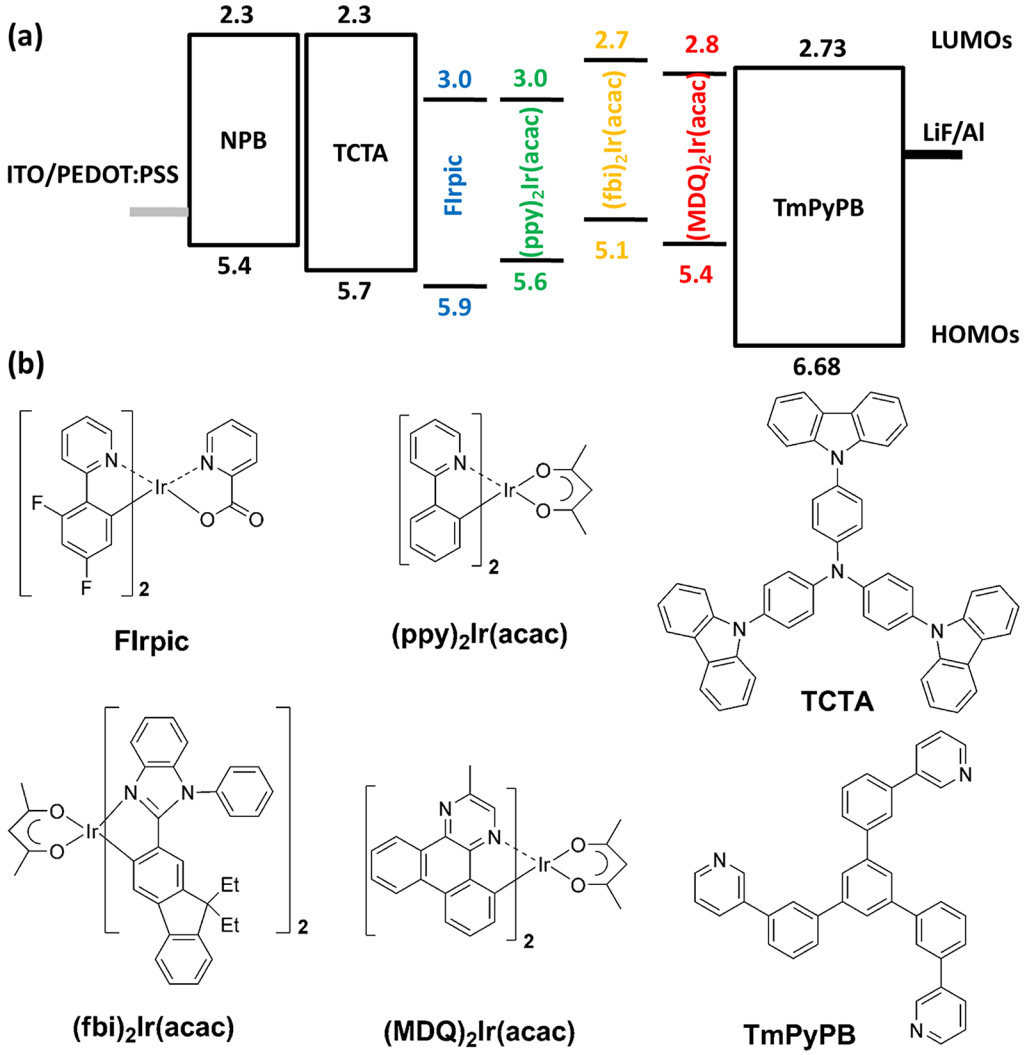

Figure 1. (a) Energy level diagram of the ultrathin nondoped EML based OLEDs. (b) Molecule structures of the phosphorescent dyes and the transporting/blocking materials.

EXPERIMENTAL SECTION

The fabricated devices were grown on cleaned glass substrates precoated by a 180 nm thickness of indium tin oxide (ITO) with a sheet resistance of 10 Ω per square. The ITO surface was treated by oxygen plasma for 2 min, following a degrease in an ultrasonic solvent bath, and then dried at 120 °C. A poly(3,4-ethylenedioxythiophene) poly(styrenesulfonate) (PEDOT:PSS; Clevios P VP AI 4083) film was formed by pin-coating at 3000 rpm and then baked at 120 °C for 30 min. Other organic layers and a metal layer were grown by thermal evaporation in a high-vacuum system with a pressure of less than 5×10^{-4} Pa without breaking the vacuum. The evaporation rates were monitored by a frequency counter and calibrated by a Dektak 6 M profiler (Veeco). The typical evaporation rate for the organic layer, LiF, and Al are 1−2, 0.1−0.2, and 10−20 Å/s, respectively. The evaporation rate for the phosphorescent dyes is 0.01−0.02 Å/s. The layer thickness for the ultrathin nondoped EML is the effective or average layer thickness as such thin film should be around or below monolayer thickness. The overlap between ITO and Al electrodes was 4 mm × 4 mm as the active emissive area of the devices. The current density−voltage (J−V) and brightness-voltage (B−V) characteristics were measured by using a Keithley source measurement unit (Keithley 2400 and Keithley 2000) with a calibrated silicon photodiode. The electroluminescence (EL) spectra were measured by a Spectrascan PR650 spectrophotometer. All the measurements were carried out in ambient atmosphere at room temperature.

RESULTS AND DISCUSSION

The phosphorescent dyes in this study are bis(3,5-difluoro-2-(2-pyridyl)phenyl-(2-carboxypyridyl)iridium III (FIrpic) for blue, bis(2-phenylpyridine)(acetylacetonate)iridium(III) [$(ppy)_2Ir(acac)$] for green, bis(2-(9,9-diethyl-9*H*-fluoren-2-yl)-1-phenyl-1*H*-benzoimidazol-*N*,C3)iridium(acetylacetonate) [$(fbi)_2Ir(acac)$] for orange, and bis(2-methyldibenzo[*f*,*h*]-quinoxaline) (acetylacetonate) iridium(III) [$(MDQ)_2Ir(acac)$] for red, as shown in Figure 1. The device structure is shown in Figure 1a, where ITO/PEDOT:PSS, *N*,*N*′-bis(naphthalen-1-yl)-*N*,*N*′-bis(phenyl)benzidine (NPB), 4,4′,4′′-tris(*N*-carbazolyl) triphenylamine (TCTA), 1,3,5-tri(m-pyrid-3-yl-phenyl)benzene (TmPyPB), and LiF/Al are used as anode, hole transporting layer, electron/exciton blocking layer, hole/exciton blocking and electron transporting layer, and cathode, respectively. From the hole transporting nature of TCTA[23] and electron transporting nature of TmPyPB,[24] it can be assumed that the main recombination zone locates at the vicinity of TCTA/TmPyPB interface. Meanwhile, due to the fact that the triplet energy levels of TCTA (2.86 eV) and TmPyPB (2.78 eV) are higher than that of all the four phosphorescent dyes, effective exciton blocking at both sides of the EML can be accomplished. As a comparison, OLEDs with

dx.doi.org/10.1021/am3026097 | ACS Appl. Mater. Interfaces 2013, 5, 965−971

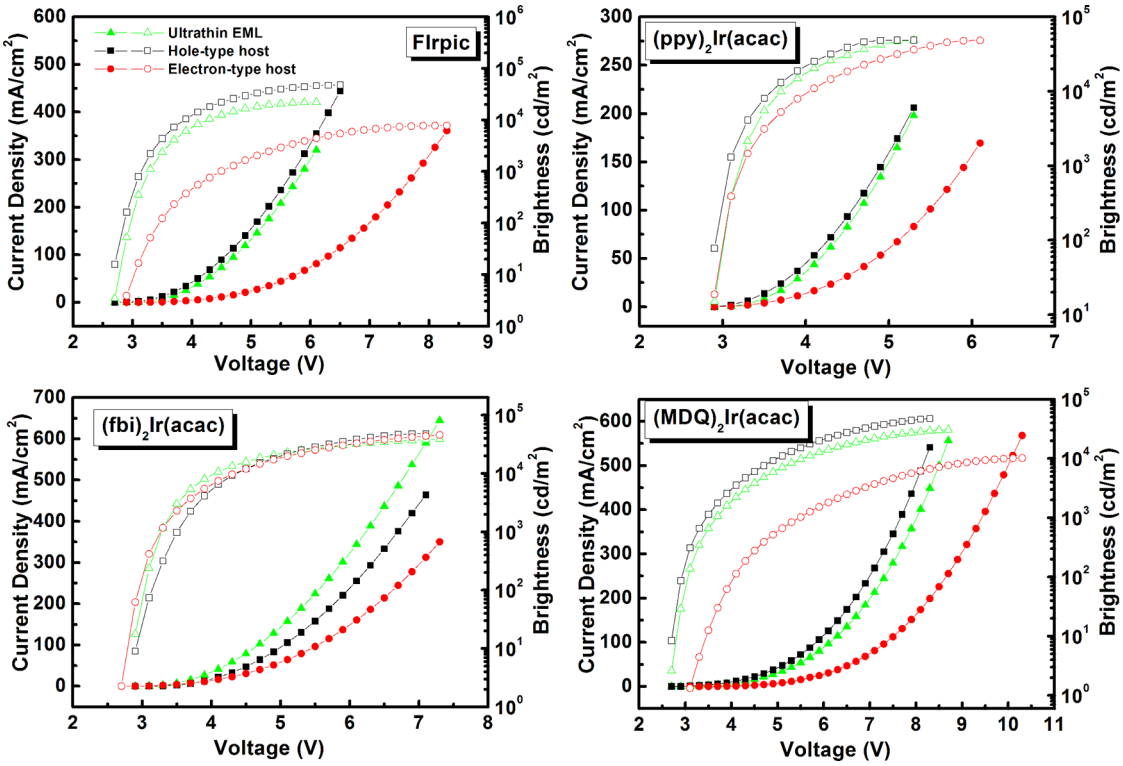

Figure 2. Current density−voltage (J−V) and brightness−voltage (B−V) characteristics of the OLEDs based on ultrathin nondoped EML, hole-type host, and electron-type host doped EMLs for FIrpic, $(ppy)_2Ir(acac)$, $(fbi)_2Ir(acac)$, and $(MDQ)_2Ir(acac)$.

Table 1. Summary of Turn on Voltage and Maximum Brightness Data of the OLEDs with structure A, B, and C

dye	V_{on}(A/B/C) [V]	maximum brightness (A/B/C) [cd/m^2]
FIrpic	2.7/2.7/2.9	22000/47000/7800
$(ppy)_2Ir(acac)$	2.7/2.7/2.7	48000/48000/48000
$(fbi)_2Ir(acac)$	2.8/2.8/2.7	38000/38000/43000
$(MDQ)_2Ir(acac)$	2.7/2.7/3.1	30000/47000/10100

doped EML were also fabricated, where the host is either TCTA or TmPyPB. Detailed device structures are:

Structure A (ultrathin EML): ITO/PEDOT:PSS (35 nm)/ NPB (40 nm)/TCTA (15 nm)/dye (0.1 nm)/TmPyPB (30 nm)/LiF (1 nm)/Al (100 nm)
Structure B (hole-type host): ITO/PEDOT:PSS (35 nm)/ NPB (40 nm)/TCTA (5 nm)/TCTA:8 wt % dye (10 nm)/TmPyPB (30 nm)/LiF (1 nm)/Al (100 nm)
Structure C (electron-type host): ITO/PEDOT:PSS (35 nm)/NPB (40 nm)/TCTA (15 nm)/ TmPyPB:8 wt % dye (10 nm)/TmPyPB (30 nm)/LiF (1 nm)/Al (100 nm)

Figure 2 shows the J−V and B−V curves of the devices with structure A, B, and C for the four dyes. As we can see, due to the approximate thickness of structure A and B, the J−V curves show marginal difference. The smaller J−V of structure C is due to the larger device thickness compared with structure A and B. All these devices show approximately the same turn on voltages of 2.7−2.8 V, except structure C with FIrpic and $(MDQ)_2Ir(acac)$ as the guest dyes, which shows relatively larger turn on voltages (2.9 V for FIrpic and 3.1 V for $(MDQ)_2Ir(acac)$), indicates the poor host−guest combination of FIrpic or $(MDQ)_2Ir(acac)$ with TmPyPB. As a result, the maximum brightness shows similar trend. The turn on voltage and maximum brightness are also summarized in Table 1.

Figure 3 and Table 2 summarize the EQE, current efficiency (CE), and power efficiency (PE) characteristics of the devices. The maximum EQEs of the devices with the structures A, B, and C are 17.1%, 19.2%, and 12.8% for FIrpic and 19.2%, 20.5%, and 13.6% for $(MDQ)_2Ir(acac)$, respectively. It is clear that in FIrpic and $(MDQ)_2Ir(acac)$ doped devices, with TCTA as the host, nearly 100% exciton utilization is realized, whereas with TmPyPB as the host the excitons cannot be effectively

Table 2. Summary of EQE, Current Efficiency, and Power Efficiency Data of the OLEDs with structure A, B, and C

	external quantum efficiency [%][c]		current efficiency [cd/A]		power efficiency [lm/W]	
dye	EQE_{MAX}[a] (A/B/C)	EQE_{1000}[b] (A/B/C)	CE_{MAX}[a] (A/B/C)	CE_{1000}[b] (A/B/C)	PE_{MAX}[a] (A/B/C)	PE_{1000}[b] (A/B/C)
FIrpic	17.1/19/12.8	15/18.1/4.3	37/41.1/26.9	33/39/8.9	43/47/29	31/38/6
$(ppy)_2Ir(acac)$	20.9/18.3/21.6	20.3/18.1/21.5	77.5/67.8/79.9	74/67.7/79.5	83/71/81	73/68/78
$(fbi)_2Ir(acac)$	17.3/15.8/20.6	16.5/14/20.2	47.5/43/57.1	45/38/56	51/45/60	43/33/53
$(MDQ)_2Ir(acac)$	19.2/20.5/13.6	18.1/20.1/4.08	29.8/32.3/20.1	28.5/32/6.6	32/34/19	24/29/4

[a]EQE_{MAX}, CE_{MAX}, and PE_{MAX} are the maximum external quantum efficiency, maximum current efficiency, and maximum power efficiency of the OLEDs. [b]EQE_{1000}, CE_{1000}, and PE_{1000} are the maximum external quantum efficiency, maximum current efficiency and maximum power efficiency of the OLEDs at a luminance of 1000 cd/m^2. [c]EQE (A/B/C) means the EQE of the OLEDs with structure A, B, and C.

dx.doi.org/10.1021/am3026097 | ACS Appl. Mater. Interfaces 2013, 5, 965−971

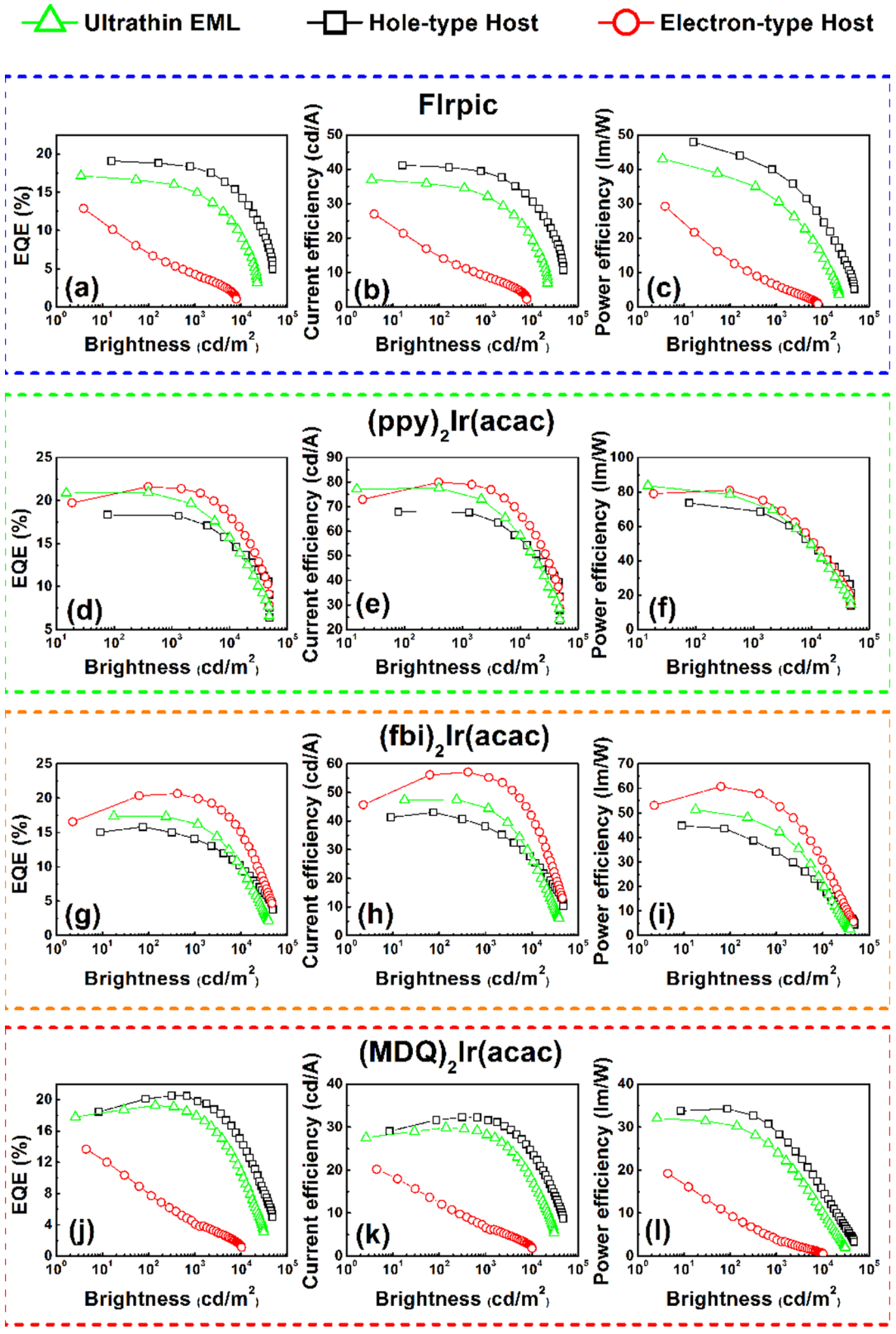

Figure 3. External quantum efficiency, current efficiency, and power efficiency of OLEDs based on ultrathin nondoped EML and hole-type host and electron-type host doped EMLs for FIrpic, $(ppy)_2Ir(acac)$, $(fbi)_2Ir(acac)$, and $(MDQ)_2Ir(acac)$.

used, indicating that the nonradiative decay of excitons or exciton quenching is more pronounced in TmPyPB than in TCTA. However, as we see, the efficiencies of the devices with ultrathin nondoped EML (structure A) were not affected by the contact of TmPyPB, the approximately same high efficiencies as device B is realized, indicating that the exciton quenching effect existed in device C is greatly suppressed. Furthermore, for the cases of $(ppy)_2Ir(acac)$ and $(fbi)_2Ir(acac)$, the devices with TmPyPB as the host show the highest efficiencies whereas with TCTA as the host there exists certain exciton quenching.

dx.doi.org/10.1021/am3026097 | ACS Appl. Mater. Interfaces 2013, 5, 965−971

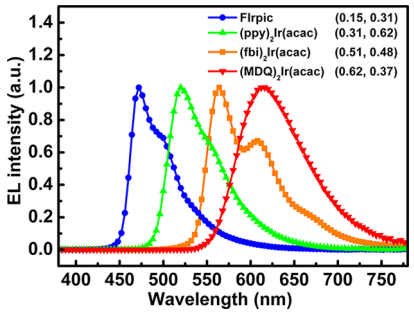

Figure 4. Electroluminescence spectra of the monochrome OLEDs with ultrathin nondoped EML.

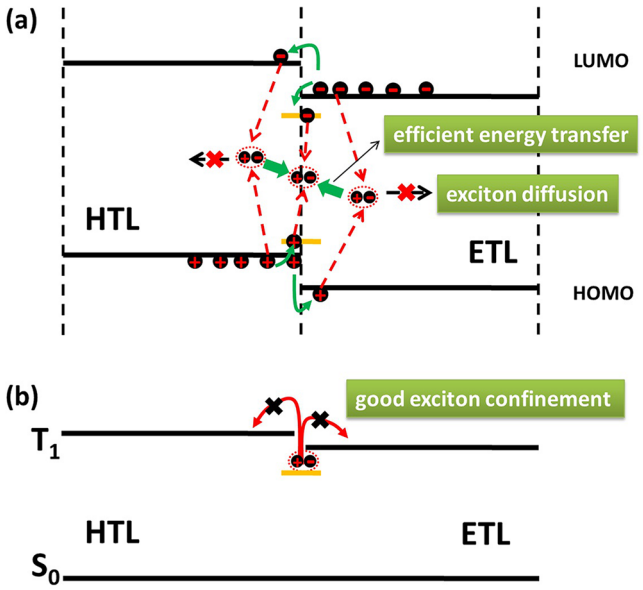

Figure 5. (a) Exciton generation, diffusion, and transfer processes at the vicinity of the ultrathin nondoped EML and (b) exciton confinement effect of the transporting layers.

Adachi et al. have reported[25] that as $(ppy)_2Ir(acac)$ was doped in an electron-type host 3-(4-biphenyl)-4-phenyl-5-*tert*-butylphenyl-1,2,4-triazole (TAZ), direct electron−hole recombination on the dopant leads to nearly 100% internal quantum efficiency. The case of TmPyPB as the host should be similar to this. More importantly, the utilization of the ultrathin nondoped EML structure yields very high efficiencies for $(ppy)_2Ir(acac)$ and $(fbi)_2Ir(acac)$. Especially, for $(ppy)_2Ir(acac)$ green dyes, EQE as high as 20.9% has been achieved and the EQE at 1000 cd/m^2 is still higher than 20%, indicating the effectivity of ultrathin nondoped EML for $(ppy)_2Ir(acac)$. The behaviors of PEs and CEs for the four dyes are similar with the EQEs.

It can be seen that the performance of the devices with doped EMLs is heavily dependent on the host materials. The improper host selection will greatly reduce device efficiency due to exciton quenching effect. As we can see, the utilization of ultrathin nondoped EML structure avoids the problem of host choice. Since all the ultrathin nondoped EML based monochrome blue, green, orange, and red OLEDs show very high efficiency, we conclude that the ultrathin nondoped EML structure has a broad adaptability for most phosphorescent dyes. As there is relatively less reports on host materials that have such broad adaptability for phosphorescent dyes, our approach provides a simple physical method to achieve this aim and thus has great potential in realizing simple and efficient OLEDs.

Figure 4 shows the electroluminescence spectra of the ultrathin nondoped EML based OLEDs for the four phosphorescent dyes. It can be seen that all the four OLEDs show pure dye emission. As depicted in Figure 5a, besides the direct charge carrier recombination on phosphorescent dyes to generate dye emission, due to the thin nature of ultrathin nondoped EML, some of electrons and holes would penetrate the EML (where the penetration depth is about 3 nm)[26] and recombine in the transporting layers. These excitons may either transfer their energy to the EML or diffuse into the transporting layer away from the EML (radiative decay may happen due to ineffective energy transfer). From the high efficiency and pure dye emission in the ultrathin nondoped EML based devices, we can infer that

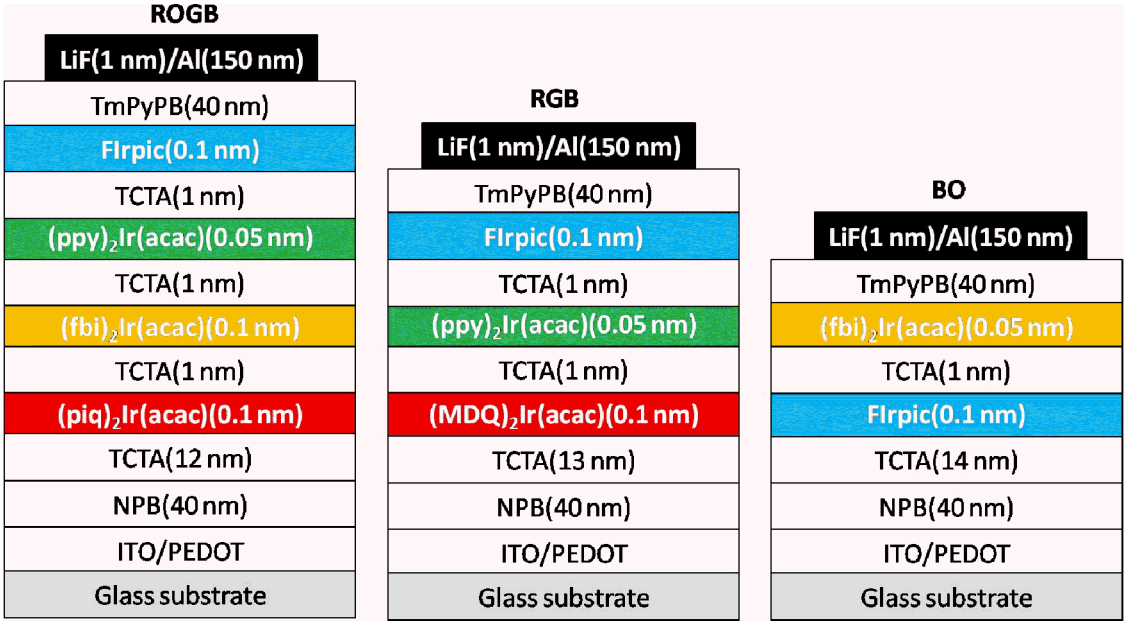

Figure 6. Device structure of the white OLEDs based on ultrathin nondoped EMLs.

dx.doi.org/10.1021/am3026097 | ACS Appl. Mater. Interfaces 2013, 5, 965−971

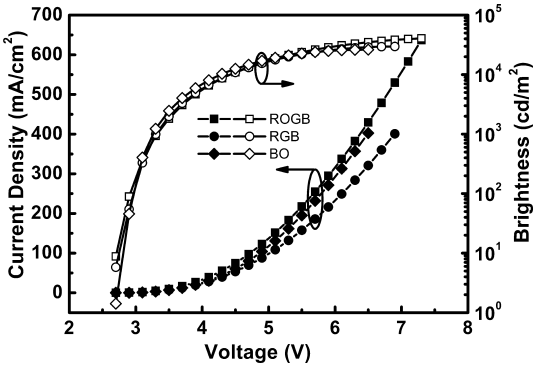

Figure 7. Current density–voltage and brightness–voltage curves of the white OLEDs based on ultrathin nondoped EMLs.

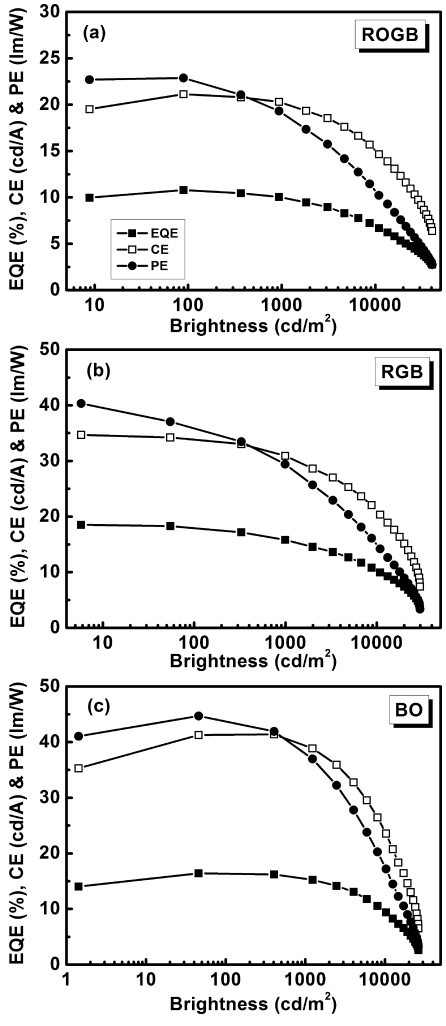

Figure 8. EQEs, CEs, and PEs of the white OLEDs based on ultrathin nondoped EMLs.

the energy transfer process from the transporting layers to the EML is much more favored than exciton diffusion. Meanwhile, due to the exciton confinement structure of heterojunction between transporting layers, the excitons generated are effectively confined in the EML (as depicted in Figure 5b).

As we know, most white OLEDs are based on thick doped EMLs. To further demonstrate the potential of the ultrathin nondoped EMLs, we fabricated several white OLEDs with only ultrathin nondoped EMLs. The device structures are shown in Figure 6. As we can see, a thin TCTA interlayer (1 nm) is inserted between different ultrathin nondoped EMLs to suppress the energy transfer between them, which is critical for realizing balanced white emission. It is obvious that all the three white OLEDs should be very easy to fabricate and the color of each device can be easily tuned by changing the TCTA interlayer thickness. The $J-V$ and $L-V$ curves for the three white OLEDs are shown in Figure 7. As we can see, all of them show similar turn on voltages and $J-V$ properties, indicating that the ultrathin nondoped EMLs have very small influence on the charge carrier transporting. The efficiencies of the three white OLEDs were shown in Figure 8 and Table 3. As we can see, the device BO and

Table 3. Summary of Device Performance of the White OLEDs Based on Ultrathin Nondoped EMLs

device	V_{on} [V]	B_{max} [a] [cd/m²]	$EQE_{Max/1000}$ [b] [%]	$CE_{Max/1000}$ [c] [cd/A]	$PE_{Max/1000}$ [d] [lm/W]
ROGB	2.7	40600	10.8/10	21.1/20	23/19
RGB	2.7	29700	18.5/15	34.6/30	40/29
BO	2.7	26200	16.4/16	41.3/40	44/37

[a]Maximum brightness of the white OLEDs. [b]Maximum external quantum efficiency and external quantum efficiency at a luminance of 1000 cd/m². [c]Maximum current efficiency and current efficiency at a luminance of 1000 cd/m². [d]Maximum power efficiency and power efficiency at a luminance of 1000 cd/m².

RGB show maximum EQE, CE, and PE of 16.4%, 41.3 cd/A, 44 lm/W and 18.5%, 34.6 cd/A, 40 lm/W, respectively, which are comparable to doped EML white OLEDs. However, for the red/orange/green/blue (ROGB) device, the maximum EQE is about 10.5%, which is mainly limited by the low efficiency of the red $(piq)_2Ir(acac)$ layer. By comparing with the EQEs at 1000 cd/m², it is obvious that all the three white OLEDs show small EQE roll-off properties. The EL spectra and the colorimetric parameters of the three devices at 1000 cd/m² are shown in Figure 9. As we can see, all of them show good white

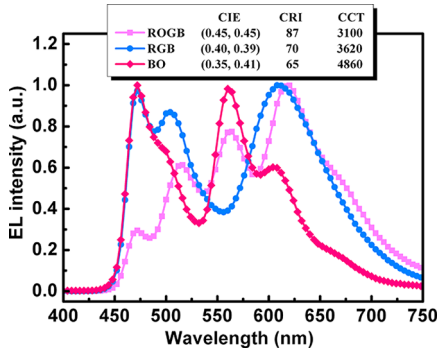

Figure 9. Electroluminance spectra of the white OLEDs based on ultrathin nondoped EMLs.

emission, while the ROGB device shows a high CRI of 87. All of above indicates that it is possible to fabricate high performance white OLEDs with ultrathin nondoped EMLs.

CONCLUSION

In conclusion, using an ultrathin nondoped phosphorescent dye layer to construct an EML is a cost-effective method to realize highly efficient OLEDs. We showed that this method possesses a wide universality for any phosphorescent dyes. It is important to optimize the transporting layers at the two sides of the EML

dx.doi.org/10.1021/am3026097 | ACS Appl. Mater. Interfaces 2013, 5, 965–971

to achieve better exciton confinement and reduce the exciton quenching, thus further improving device performance. We also showed that high performance full color white OLEDs can be realized with only ultrathin nondoped EMLs in a simple way. We believe that this approach should offer high values in the future practical application as a result of wise material choice.

AUTHOR INFORMATION

Corresponding Author

*E-mail: mdg1014@ciac.jl.cn.

Notes

The authors declare no competing financial interest.

ACKNOWLEDGMENTS

The authors thank the Science Fund for Creative Research Groups of NSFC (20921061), the National Natural Science Foundation of China (50973104, 60906020, 61036007, 60937001), Ministry of Science and Technology of China (973 program No. 2009CB623604, 2009CB930603), and the Foundation of Jilin Research Council (201105028, 20090127) for the support of this research.

REFERENCES

(1) Tang, C. W.; VanSlyke, S. A. *Appl. Phys. Lett.* **1987**, *51*, 913−915.
(2) Forrest, S. R. *Org. Electron.* **2003**, *4*, 45−48.
(3) D'Andrade, B. W.; Forrest, S. R. *Adv. Mater.* **2004**, *16*, 1585−1595.
(4) Forrest, S. R. *Nature* **2004**, *428*, 911−918.
(5) So, F.; Kido, J.; Burrows, P. *MRS Bull.* **2008**, *33*, 663−669.
(6) Tang, C. W.; VanSlyke, S. A.; Chen, C. H. *J. Appl. Phys.* **1989**, *65*, 3610−3616.
(7) Hung, L.; Tang, C. W.; Mason, M. *Appl. Phys. Lett.* **1997**, *70*, 152−154.
(8) You, H.; Dai, Y. F.; Zhang, Z. Q.; Ma, D. G. *J. Appl. Phys.* **2007**, *101*, 026105.
(9) Baldo, M. A.; O'Brien, D. F.; You, Y.; Shoustikov, A.; Sibley, S.; Thompson, M. E.; Forrest, S. R. *Nature* **1998**, *395*, 151−154.
(10) Huang, J.; Pfeiffer, M.; Werner, A.; Blochwitz, J.; Leo, K.; Liu, S. *Appl. Phys. Lett.* **2002**, *80*, 139−141.
(11) Pfeiffer, M.; Forrest, S. R.; Leo, K.; Thompson, M. E. *Adv. Mater.* **2002**, *14*, 1633−1636.
(12) Kido, J.; Matsumoto, T. *Appl. Phys. Lett.* **1998**, *73*, 2866−2868.
(13) Parthasarathy, G.; Shen, C.; Kahn, A.; Forrest, S. R. *J. Appl. Phys.* **2001**, *89*, 4986−4992.
(14) Goushi, K.; Kwong, R.; Brown, J. J.; Sasabe, H.; Adachi, C. *J. Appl. Phys.* **2004**, *95*, 7798−7802.
(15) Su, S. J.; Gonmori, E.; Sasabe, H.; Kido, J. *Adv. Mater.* **2008**, *20*, 4189−4194.
(16) Sun, Y. R.; Forrest, S. R. *Nat. Photon.* **2008**, *2*, 483−487.
(17) Reineke, S.; Lindner, F.; Schwartz, G.; Seidler, N.; Walzer, K.; Lussem, B.; Leo, K. *Nature* **2009**, *459*, 234−238.
(18) Kim, S. Y.; Jeon, W. S.; Park, T. J.; Pode, R.; Jang, J.; Kwon, J. H. *Appl. Phys. Lett.* **2009**, *94*, 133303.
(19) Liu, Z.; Helander, M. G.; Wang, Z. B.; Lu, Z. H. *Org. Electron.* **2009**, *10*, 1146−1151.
(20) Divayana, Y.; Sun, X. W. *Org. Electron.* **2009**, *10*, 320−325.
(21) Liu, S.; Li, B.; Zhang, L.; Song, H.; Jiang, H. *Appl. Phys. Lett.* **2010**, *97*, 083304.
(22) Zhao, Y. B.; Chen, J. S.; Ma, D. G. *Appl. Phys. Lett.* **2011**, *99*, 163303.
(23) Kuwabara, Y.; Ogawa, H.; Inada, H.; Noma, N.; Shirota, Y. *Adv. Mater.* **1994**, *6*, 677−679.
(24) Su, S. J.; Chiba, T.; Takeda, T.; Kido, J. *Adv. Mater.* **2008**, *20*, 2125−2130.
(25) Adachi, C.; Baldo, M. A.; Thompson, M. E.; Forrest, S. R. *J. Appl. Phys.* **2001**, *90*, 5048−5051.
(26) Zhao, Y. B.; Zhu, L. P.; Chen, J. S.; Ma, D. G. *Org. Electron.* **2012**, *13*, 1340−1348.